NeuroImage 48 (2009) 362–370

Contents lists available at ScienceDirect

NeuroImage

journal homepage: www.elsevier.com/locate/ynimg

Quantitation of cannabinoid CB_1 receptors in healthy human brain using positron emission tomography and an inverse agonist radioligand

Garth E. Terry [a,c], Jeih-San Liow [a], Sami S. Zoghbi [a], Jussi Hirvonen [a], Amanda G. Farris [a], Alicja Lerner [a], Johannes T. Tauscher [b], John M. Schaus [b], Lee Phebus [b], Christian C. Felder [b], Cheryl L. Morse [a], Jinsoo S. Hong [a], Victor W. Pike [a], Christer Halldin [c], Robert B. Innis [a,*]

[a] Molecular Imaging Branch, National Institute of Mental Health, Bethesda, MD, USA
[b] Lilly Research Laboratories, Lilly Corporate Center, Indianapolis, IN, USA
[c] Karolinska Institutet, Department of Clinical Neuroscience, Psychiatry Section, Stockholm, Sweden

ARTICLE INFO

Article history:
Received 20 March 2009
Revised 21 May 2009
Accepted 20 June 2009
Available online 30 June 2009

Keywords:
Positron emission tomography
Brain imaging
Neuroimaging

ABSTRACT

[^{11}C]MePPEP is a high affinity, CB_1 receptor-selective, inverse agonist that has been studied in rodents and monkeys. We examined the ability of [^{11}C]MePPEP to quantify CB_1 receptors in human brain as distribution volume calculated with the "gold standard" method of compartmental modeling and compared results with the simple measure of brain uptake. A total of 17 healthy subjects participated in 26 positron emission tomography (PET) scans, with 8 having two PET scans to assess retest variability. After injection of [^{11}C]MePPEP, brain uptake of radioactivity was high (*e.g.*, 3.6 SUV in putamen at ~60 min) and washed out very slowly. A two-tissue compartment model yielded values of distribution volume (which is proportional to receptor density) that were both well identified (SE 5%) and stable between 60 and 210 min. The simple measure of brain uptake (average concentration of radioactivity between 40 and 80 min) had good retest variability (~8%) and moderate intersubject variability (16%, coefficient of variation). In contrast, distribution volume had two-fold greater retest variability (~15%) and, thus, less precision. In addition, distribution volume had three-fold greater intersubject variability (~52%). The decreased precision of distribution volume compared to brain uptake was likely due to the slow washout of radioactivity from brain and to noise in measurements of the low concentrations of [^{11}C]MePPEP in plasma. These results suggest that brain uptake can be used for within subject studies (*e.g.*, to measure receptor occupancy by medications) but that distribution volume remains the gold standard for accurate measurements between groups.

Published by Elsevier Inc.

Introduction

Cannabinoid CB_1 receptors, which mediate the psychotropic actions of marijuana, are widely distributed in brain and may well be the most abundant G protein coupled receptor in brain (for review see Howlett et al., 2002). CB_1 receptors are primarily located presynaptically and inhibit the release of several neurotransmitters, including GABA, glutamate, and dopamine. Endogenous transmitters (*i.e.*, "endocannabinoids" such as anandamide and 2-arachidonylglycerol) are released from postsynaptic sites and act via "retrograde neurotransmission" on presynaptically located CB_1 receptors. The CB_1 receptor is thought to have an important role in normal physiology (*e.g.*, appetite and memory) and may be involved in the pathophysiology of some neuropsychiatric (schizophrenia) (Eggan et al., 2008) and metabolic (obesity) disorders (Gazzerro et al., 2007). Until recently, the CB_1 receptor has been an active target of drug development. Clinical research and/or use of two inverse agonists (rimonabant and taranabant) were discontinued in 2008 because of psychiatric side effects (depression, anxiety, and suicidal thoughts) (Jones, 2008).

Development of a positron emission tomographic (PET) radioligand for the CB_1 receptor has been difficult, primarily because of the high lipophilicity of the available ligands. High lipophilicity tends to cause high nonspecific retention in the abundant fat of brain and also causes high binding to plasma proteins, the latter of which limits access of the radioligand to brain. High lipophilicity likely caused the failure of two early radioligands, which had either high nonspecific binding in brain or low delivery to brain (Gatley et al., 1996; Gatley et al., 1998). More recently, three PET radioligands have successfully imaged CB_1 receptors in monkey and/or human brain: [^{18}F]MK-9470 (Burns et al., 2007), [^{11}C]JHU75528 (Horti et al., 2006; Wong et al., 2008), and [^{11}C]MePPEP (Yasuno et al., 2008). Results quantified with the "gold standard" method of compartmental modeling using concurrent brain and plasma data have been fully reported only for [^{11}C]MePPEP, and that quantitation was done only in animals. Furthermore, prior studies of [^{18}F]MK-9470 in human subjects quantified CB_1 receptors using only brain uptake, without correction

* Corresponding author. National Institute of Mental Health, 31 Center Drive, Bethesda, MD 20892-2035, USA.
E-mail address: robert.innis@nih.gov (R.B. Innis).

1053-8119/$ – see front matter. Published by Elsevier Inc.
doi:10.1016/j.neuroimage.2009.06.059

for the concentration of radioligand in plasma. Thus, the current study also evaluated the accuracy and precision of brain uptake as a proxy for distribution volume calculated with compartmental modeling.

MePPEP has high affinity ($K_D = 0.14$ nM in human cerebellum; unpublished data) and selectivity for the CB_1 receptor (Terry et al., 2008; Yasuno et al., 2008). The majority of brain uptake (65 to 85%) in mice, rats, and monkeys represents specific binding to CB_1 receptors. Specific binding was determined by pharmacological blockade or by genetic knockout of the CB_1 receptor. Receptor binding in both rat and monkey was quantified with compartmental modeling, using serial measurements of both radioactivity in brain and the concentration of unchanged parent radioligand in plasma.

Similar to our prior experiments in rat and monkey brain, we sought in the current study to evaluate [^{11}C]MePPEP in healthy human brain using compartmental modeling. The outcome measure was total distribution volume (V_T), which equals the ratio at equilibrium of radioactivity in brain to the concentration of parent radioligand in plasma. We scanned eight subjects for 150 min and found that the intersubject variability (coefficient of variation, COV) of V_T was higher than that of brain uptake, and higher than that of other commonly used PET tracers (10–20%). To evaluate the cause for the high variability in V_T, we measured the retest variability within subjects to separately assess the reproducibility of brain and plasma data. We also wondered if a longer acquisition time would provide better identifiability and smaller intersubject variability of V_T. Therefore, we scanned for a longer time and surprisingly found that meaningful brain data were still provided at 210 min using a radioligand labeled with ^{11}C, which has a half-life of only 20.4 min.

Methods

Radioligand preparation

[^{11}C]MePPEP ((*3R,5R*)-5-(3-methoxy-phenyl)-3-((*R*)-1-phenyl-ethylamino)-1-(4-trifluoromethyl-phenyl)-pyrrolidin-2-one) was prepared by [^{11}C]methylation of its desmethyl analogue with [^{11}C]-iodomethane (Donohue et al., 2008). The preparation is described in detail in our Investigational New Drug Application #79,948, submitted to the US Food and Drug Administration and a copy of which is available at http://pdsp.med.unc.edu/snidd/. The radioligand was obtained in high radiochemical purity (>99%) and had specific radioactivity at time of injection of 81 ± 40 GBq/μmol ($n = 26$ batches).

Human subjects

Eight healthy subjects (4 females and 4 males; age, 38 ± 12 years; body weight, 71 ± 18 kg) participated in the initial studies lasting 150 min. Ten healthy subjects (4 females and 6 males; age 27 ± 5 years; body weight, 78 ± 13 kg) participated in studies lasting 210 min, with 8 subjects completing retest studies. One of these subjects participated in a 150 minute study as well as the 210 minute retest studies; therefore, 17 subjects were studied in total. All subjects were free of current medical and psychiatric illness based on history, physical examination, electrocardiogram, urinalysis including drug screening, and blood tests (complete blood count, serum chemistries, thyroid function test, and antibody screening for syphilis, HIV, and hepatitis B). The subjects' vital signs were recorded before [^{11}C]MePPEP injection and at 15, 30, 90, and 120 min after injection. Subjects returned to repeat urinalysis and blood tests about 24 h after the PET scan.

PET scans

After injection of [^{11}C]MePPEP (636 ± 120 MBq) in the eight initial subjects, dynamic PET scans were acquired in 3D mode with a GE Advance camera (GE Healthcare; Waukesha, WI) for 150 min in 39 frames of increasing duration from 30 s to 5 min. After injection of [^{11}C]MePPEP (657 ± 76 MBq) in the other ten subjects, dynamic PET scans were acquired over 210 min in two 90 minute sessions, consisting of 45 frames of increasing duration from 30 s to 5 min; subjects were allowed a 30 minute rest period outside the camera between the two sessions. Data were reconstructed with 3D filtered back-projection and a Hanning filter, resulting in an image resolution of 7.0 mm full width at half maximum. All PET images were corrected for attenuation and scatter. Head movement was restricted with a thermoplastic mask and was further corrected by intrasubject alignment during reconstruction. Subjects participating in the retest studies had the test scan in the morning and the retest scan in the afternoon.

Measurement of [^{11}C]MePPEP in plasma

Blood samples (1 mL each) were drawn from the radial artery at 15 second intervals until 2 min, followed by 3 mL samples at 3, 5, 10, 20, 30, 45, and 60 min, and 6 mL samples at 75, 90, and 120 min. The plasma time-activity curve was corrected for the fraction of unchanged radioligand by radio-HPLC separation, as previously described (Imaizumi et al., 2007).

The plasma free fraction of [^{11}C]MePPEP was measured by ultrafiltration through Centrifree membrane filters, as previously described (Gandelman et al., 1994). Plasma samples from each subject were stored in a −70 °C freezer, and free fractions were measured on a day other than the PET scan. Measurements were performed either two or three times for each sample with batches of plasma samples receiving a common preparation of [^{11}C]MePPEP each time. The formulation of [^{11}C]MePPEP that was used to measure plasma free fraction did not contain Tween 80, which may affect plasma protein binding and whose presence would not be representative of *in vivo* conditions.

Image analysis

PET images were spatially normalized to a standard anatomic orientation (Montreal Neurological Institute, or MNI, space) based on transformation parameters from a magnetic resonance image (MRI). Either 1.5 T (1.2 mm per slice) or 3.0 T (1.0 mm per slice) axial MRIs were obtained using spoiled gradient recall acquisition in the steady state protocol. First, the summed PET image of all time frames was coregistered to the MRI of the individual subject using a 6-parameter algorithm. Second, the individual's MRI was coregistered to the template MRI in MNI space using a 12-parameter algorithm. The coregistration information from the PET to subject MRI and from the subject MRI to template MRI were combined and applied to resample the individual's dynamic PET image into MNI space in a single step. All coregistration and spatial normalization of images were performed using the FSL Library (FMRIB Software Library; Oxford, UK). Normalizing PET images to the MNI template allowed use of a set of predefined volumes of interest from the automated anatomical labeling (AAL) atlas (Tzourio-Mazoyer et al., 2002). Six regions were defined from these preset volumes and analyzed: prefrontal cortex (303 cm^3), occipital cortex (172 cm^3), hippocampus including parahippocampus (32 cm^3), putamen (17 cm^3), thalamus (17 cm^3), and cerebellum (171 cm^3). Two additional regions, pons (6.5 cm^3) and white matter (8.3 cm^3), were not available from the AAL atlas, and thus were manually drawn on the MNI template and added to the AAL library of predefined volumes.

Concentration of radioactivity in brain was normalized for injected dose and body weight, and expressed as standardized uptake value (SUV).

Calculation of distribution volume using metabolite-corrected input function

The input function was analyzed as linear interpolation of the concentrations of [^{11}C]MePPEP in arterial plasma before the peak, and a tri-exponential fit of concentrations after the peak. Rate constants (K_1, k_2, k_3, and k_4) in standard one- and two-tissue compartment models (Innis et al., 2007) were calculated with weighted least squares and the Marquardt optimizer. Brain data of each frame were weighted by assuming that the standard deviation of the data is proportional to the inverse square root of noise equivalent counts. To correct the brain data for its vascular component, radioactivity in serial whole blood was measured and subtracted from the PET measurements, assuming that cerebral blood volume is 5% of total brain volume. Image and kinetic analyses were performed using PMOD 2.95 (pixel-wise modeling software; PMOD Technologies Ltd., Zurich, Switzerland) (Burger et al., 1998).

To determine the minimum scanning time necessary to obtain stable values of distribution volume, we analyzed the PET data from each subject after removing variable durations of the terminal portion of the scan. We analyzed brain data of all subjects from 0–30 min to 0–150 or 0–210 min, depending on the total acquisition length, with 10 minute decrements.

Statistical analysis

Goodness-of-fit by the compartment models was compared with F statistics (Hawkins et al., 1986). A value of $P<0.05$ was considered significant. Goodness-of-fit by nonlinear least squares analysis was evaluated using the Akaike Information Criterion (AIC) (Akaike, 1974) and the model selection criteria (MSC). The most appropriate model is that with the smallest AIC and the largest MSC values.

The identifiability of the kinetic variables was calculated as the standard error, which reflects the diagonal of the covariance matrix (Carson, 1986). Identifiability was expressed as a percentage and equals the ratio of the standard error to the rate constant itself. A lower percentage indicates better identifiability. Identifiability of V_T was calculated from the covariance matrix using the generalized form of error propagation equation (Bevington and Robinson, 2003), where correlations among the rate constants were taken into account.

Group data are expressed as mean ± SD. Group analysis of brain data does not include white matter, as it does not contain significant amounts of CB_1 receptors. The variability between subjects or intersubject variability (COV) was calculated as SD divided by the mean.

The retest variability of scans within a single subject was defined as the absolute difference between the test and retest studies, divided by the mean of the two. Intraclass correlation coefficient (ICC) was calculated for retest studies and compares the relative variation within subjects to between subjects. Values of ICC were calculated by (BSMSS − WSMSS) / (BSMSS + WSMSS), where BSMSS = mean of summed squares between subjects, and WSMSS = mean of summed squares within subjects. Values between 0 and 1 indicate that variability is higher between subjects than within subjects; values close to 1 suggest good reliability. Values between −1 and 0 indicate that variability is higher within subjects than between subjects and suggest poor reliability.

Results

Pharmacological effects

[^{11}C]MePPEP caused no pharmacological effects based on subjective reports, electrocardiogram, blood pressure, pulse, and respiration rate. In addition, no effects were noted in any of the blood and urine tests acquired about 24 h after radioligand injection. The injected radioactivity of [^{11}C]MePPEP was 651 ± 90 MBq, which corresponds to 9.4 ± 3.3 nmol of MePPEP (n = 26 injections in 17

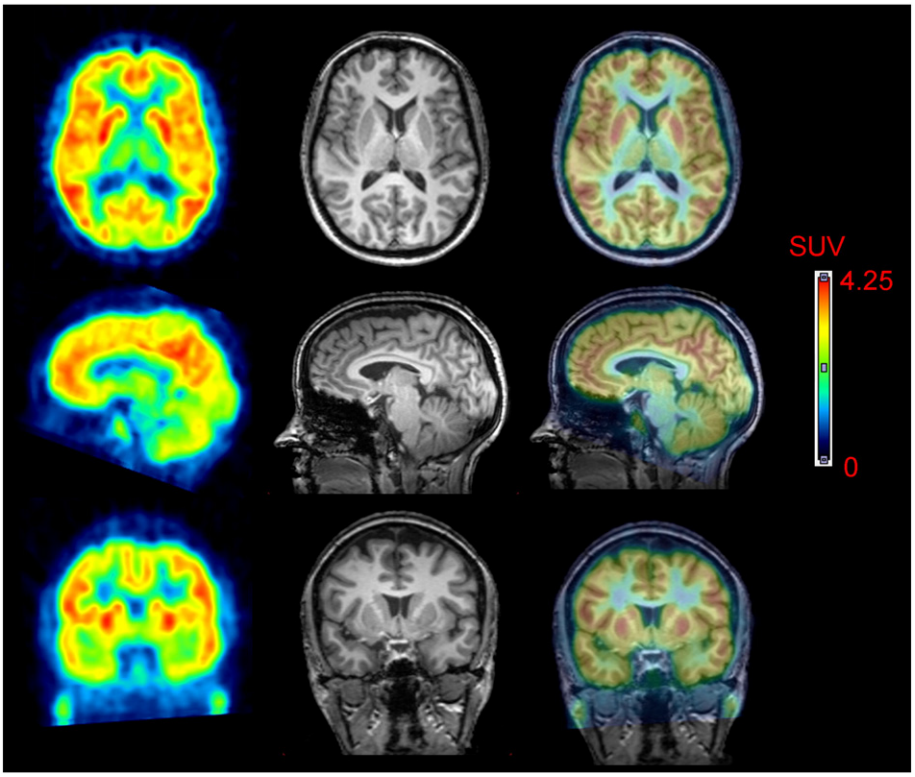

Fig. 1. [^{11}C]MePPEP in human brain. PET images from 40 to 80 min after injection of [^{11}C]MePPEP were averaged (left column) and coregistered to the subject's MRI (middle column). PET and MR images are overlaid in the right column.

subjects). Thus, an uptake of 4 SUV in brain would correspond to a receptor occupancy of 0.3%, assuming the B_{max} is 1.81 pmol/mg protein in brain (Abood et al., 1997) and that all MePPEP in brain were bound to CB_1 receptors.

Brain imaging

After injection of [^{11}C]MePPEP, all subjects showed high concentrations of radioactivity in brain that decreased slowly over time. Radioactivity in brain peaked by 60 min and was ~3.0 SUV for all areas of neocortex (Figs. 1 and 2). Areas with a high density of CB_1 receptors (*e.g.*, putamen) had an even greater concentration of radioactivity, peaking over 4.0 SUV in some subjects. Radioactivity in brain decreased slowly, remaining within ~10% of the peak by 2.5 h and within ~20% of the peak by 3.5 h. We averaged radioactivity concentration from 40 to 80 min after injection to represent brain uptake (brain uptake$_{40–80}$; Tables 1 and 3).

Two regions of the brain consistently demonstrated less uptake of radioactivity than other regions. The first region, pons, had peak uptake of ~2.2 SUV at 16 ± 10 min. After the peak, washout of radioactivity from the pons was 1.5 to 2 times faster than other regions from 60 to 150 min after injection. The second region, white matter, typically peaked at ~1.5 SUV about 30 min after injection and remained constant until the end of the scan.

Plasma analysis

The concentration of [^{11}C]MePPEP in arterial plasma peaked at 1–2 min, and then rapidly declined because of distribution in the body, followed by a slow terminal phase of clearance. To quantify the exposure of brain to [^{11}C]MePPEP, we fit the concentration of [^{11}C]MePPEP after its peak to a tri-exponential curve (Fig. 3A). Of the three associated half-lives, the first two (~0.6 and 6.7 min) largely reflected distribution, and the last (~3700 min) reflected clearance (*i.e.*, metabolism and elimination). The long value of this last half-life accounted for ~55% of the total area under the curve integrated to infinity.

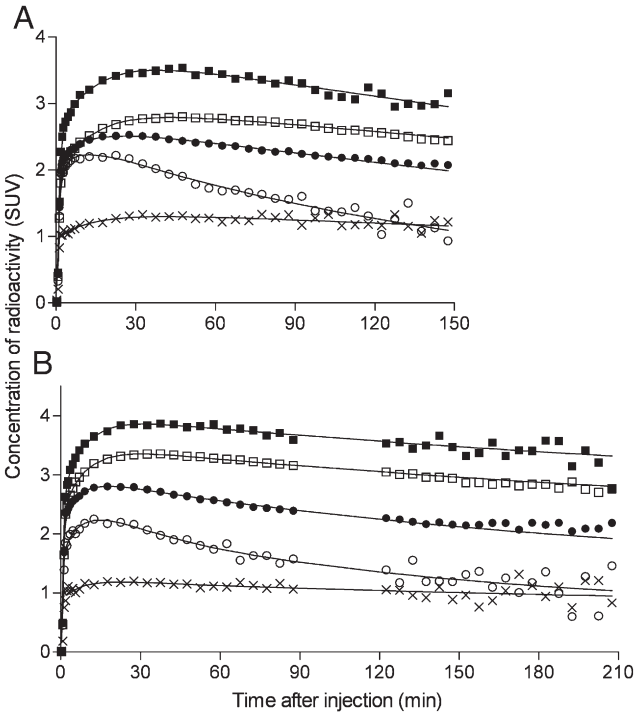

Fig. 2. Time–activity curves of [^{11}C]MePPEP in brain from different subjects scanned for (A) 150 min and (B) 210 min. Decay-corrected measurements from the putamen (■), prefrontal cortex (□), cerebellum (●), pons (○), and white matter (x) were fitted with an unconstrained 2-tissue compartment model (—). Putamen was consistently the region of highest brain uptake. White matter was consistently the region of lowest brain uptake, followed by pons. Concentration is expressed as standardized uptake value (SUV), which normalizes for injected activity and body weight.

Table 1
Brain uptake and distribution volume in 17 subjects using 150 min of scanning data.

Region	Brain uptake$_{40–80}$[a]		Distribution volume: 150 min	
	Conc. (SUV)	Intersubject variability	V_T (mL·cm^{-3}) SE	Intersubject variability
Prefrontal cortex	2.89	17%	22.4 ± 12.8 3%	57%
Occipital cortex	2.96	17%	14.6 ± 6.1 2%	42%
Hippocampus	2.26	13%	26.8 ± 23.2 7%	57%
Putamen	3.59	15%	29.1 ± 17.4 5%	60%
Thalamus	2.42	17%	11.2 ± 5.0 3%	44%
Cerebellum	2.55	16%	14.4 ± 6.8 3%	47%
Pons	1.94	18%	7.2 ± 4.0 6%	56%
White matter	1.19	16%	11.4 ± 8.4 21%	73%

Brain uptake and V_T (mean ± SD) came from 7 subjects scanned for only 150 min and from 10 subjects scanned for 210 min in the retest study. For the latter, we used only 150 min of the baseline scan.
The identifiability of V_T is inversely related to the standard error (SE). For each brain region, the SE is expressed as percent and is listed below the variable itself.
Intersubject variability is the SD divided by the mean, and is expressed as percent.
[a] Brain uptake is the average concentration of radioactivity from 40 to 80 min after injection.

Several radiometabolites of [^{11}C]MePPEP appeared in plasma (Figs. 3B, C). The main radiometabolite eluted earlier than [^{11}C]MePPEP on reverse phase HPLC and was, therefore, less lipophilic than the parent compound. The concentration of this radiometabolite peaked within 20 min and declined for the remainder of the scan. Other radiometabolites were detected throughout the scan in varying concentrations and with varying elution times on HPLC. One of these radiometabolites (Fig. 3C, metabolite F) eluted later than [^{11}C]MePPEP and was, therefore, more lipophilic than the parent compound. This radiometabolite was only apparent during part of the scan and never accounted for more than 3% of radioactivity in plasma. After 60 min, [^{11}C]MePPEP remained at about 12% of total radioactivity in plasma.

The free fraction of [^{11}C]MePPEP in plasma (f_P) was very low. The average f_P was 0.05% ± 0.01% in 12 subjects. In the retest study, f_P from morning and afternoon plasma samples were identical (expressed as a second decimal of a percent) for each subject.

Kinetic analysis based on 150 min of scan data

For this kinetic analysis, we combined results from 8 subjects who were scanned once for 150 min with the baseline scan of 10 subjects who were scanned for 210 min. The subject who was in both studies was included only once in the analysis.

The unconstrained two-tissue compartment model provided a significantly better fit of the data in all subjects than did the one-tissue compartment model, consistent with the presence of both specific and nonspecific binding in brain. Although the one-tissue model estimated K_1, k_2, and V_T with reasonable identifiability (SE 1%–6%), the curves significantly deviated from the measured brain data, especially in regions with low CB_1 receptor density. Compared to the one-tissue model, the two-tissue model had a statistically better fit to measured data by *F*-test ($P<0.05$), lower AIC scores (197 *vs.* 248, on average), and higher MSC scores (4.0 *vs.* 2.6, on average) for all brain regions.

For the two-tissue compartment model, we assessed the utility of constraining nondisplaceable uptake ($V_{ND} = K_1/k_2$) to a single value

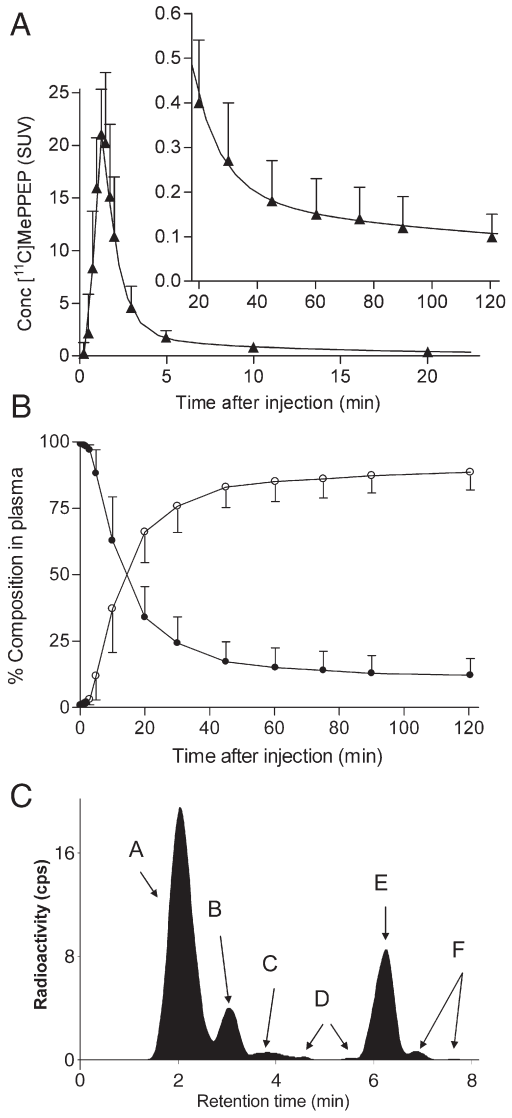

Fig. 3. Concentration of [^{11}C]MePPEP and its percentage composition in arterial plasma. (A) Average concentration of [^{11}C]MePPEP in arterial plasma from 17 subjects is plotted over time after injection. Data after the peak (about 1 min) were fitted to a tri-exponential curve (—). Symbols (▲) and error bars represent mean and SD. (B) Percent composition of parent radioligand (●) and radiometabolites (○) in arterial plasma from 17 subjects are plotted over time after injection. After 60 min, [^{11}C]MePPEP accounted for ≤15% of radioactivity in arterial plasma. (C) This radiochromatogram illustrates plasma composition from one subject, 30 min after injection of [^{11}C]MePPEP. Radioactivity was measured in counts per second (cps). Peaks are labeled with increasing lipophilicity from A to F. Peak E represents [^{11}C]MePPEP. cps = counts per second.

determined from all regions except white matter. When compared by *F*-test, the unconstrained model fit the data significantly better than did the constrained model in the majority of regions, and the AIC and MSC scores favored the unconstrained model. For these reasons, we used the unconstrained two-tissue compartment model for additional analyses.

After 150 min of scanning, the value of K_1 in all regions except white matter for all subjects ranged from 0.07 to 0.10 mL·cm^{-3}·min^{-1}, with an average of 0.09 mL·cm^{-3}·min^{-1} (Table 2). Assuming that cerebral blood flow is ~0.5 mL·cm^{-3}·min^{-1}, the extraction fraction (extraction = K_1 / flow) of [^{11}C]MePPEP from plasma to brain was ~18%. The value of k_2 in all regions except white matter ranged from 0.05 to 0.17 min^{-1}, with an average of ~0.11 min^{-1}. Thus, the value of nondisplaceable distribution volume ($V_{ND} = K_1 / k_2$) was ~2.1 mL·cm^{-3}. The value of k_3, which is defined as $k_{on} \cdot B_{max} \cdot f_{ND}$, ranged from 0.177 to 0.385 min^{-1}, with an average value of ~0.276 min^{-1}. The value of k_4, which is the dissociation rate constant from the specific compartment, was low and ranged from 0.011 to 0.046 min^{-1}, with an average of ~0.027 min^{-1}. Finally, the estimated ratio of specific to nondisplaceable uptake ($BP_{ND} = k_3 / k_4$) was ~19 in healthy human brain.

Table 2
Kinetic rate constants from the unconstrained two-compartment model in 17 subjects using 150 min of scanning data.

Region	Rate constant			
	K_1 (mL·cm^{-3} min^{-1}) SE	k_2 (min^{-1}) SE	k_3 (min^{-1}) SE	k_4 (min^{-1}) SE
Prefrontal cortex	0.08 ± 0.02 4%	0.07 ± 0.09 79%	0.385 ± 0.521 40%	0.046 ± 0.076 59%
Occipital cortex	0.10 ± 0.03 4%	0.13 ± 0.17 29%	0.341 ± 0.368 21%	0.025 ± 0.012 13%
Hippocampus	0.07 ± 0.02 4%	0.15 ± 0.15 29%	0.326 ± 0.286 18%	0.011 ± 0.007 15%
Putamen	0.10 ± 0.02 5%	0.07 ± 0.08 90%	0.293 ± 0.268 74%	0.033 ± 0.042 42%
Thalamus	0.08 ± 0.02 4%	0.09 ± 0.08 25%	0.212 ± 0.176 24%	0.026 ± 0.017 12%
Cerebellum	0.09 ± 0.02 3%	0.10 ± 0.11 16%	0.198 ± 0.160 13%	0.018 ± 0.010 8%
Pons	0.08 ± 0.02 7%	0.17 ± 0.43 33%	0.177 ± 0.248 35%	0.028 ± 0.017 22%
White matter	0.03 ± 0.01 11%	0.04 ± 0.04 403%	0.267 ± 0.501 122%	0.059 ± 0.129 461%

The subject sample is the same as for Table 1: 7 subjects scanned for 150 min and 10 subjects scanned for 210 min in the retest study. For the latter, we used only the initial 150 min of the baseline scan.
The identifiability of rate constants is inversely related to the standard error (SE). For each brain region, the SE is expressed as percent and is listed below the variable itself. Values are mean ± SD.

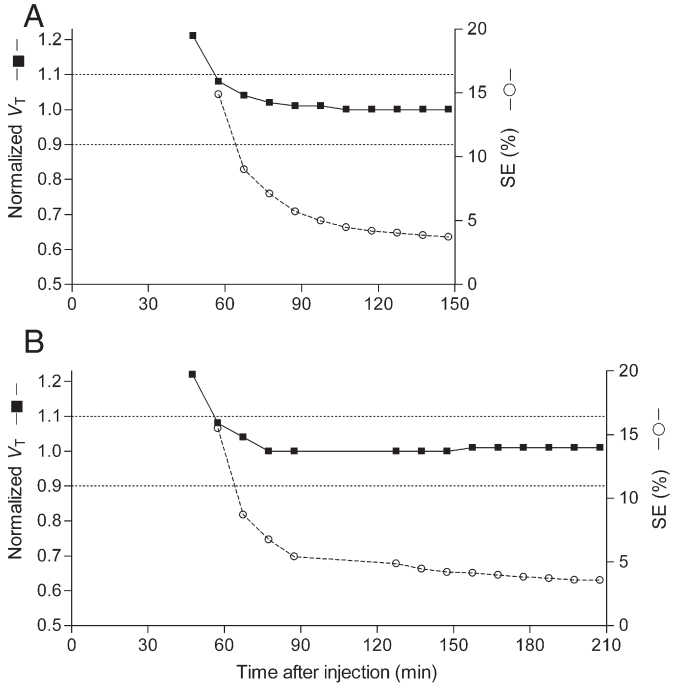

Fig. 4. Value of distribution volume (V_T) and its identifiability as function of duration of image acquisition for putamen, a high binding region. V_T (■) was calculated using an unconstrained two-tissue compartment model with increasingly truncated acquisition times. Values are normalized to the value attained with 150 min of imaging and are plotted with the *y*-axis on left. The corresponding SE (○), which is inversely proportional to identifiability, is plotted with the *y*-axis on right. (A) The points represent an average of 15 subjects scanned for a total of 150 min. Two subjects scanned for only 150 min had a slow washout, and did not have stable measurements of V_T until 120 min. (B) The points represent an average of 10 subjects scanned for a total of 210 min. Other brain regions demonstrated similar or better stability over time.

To determine the minimal scanning time necessary to obtain stable values of V_T, we calculated V_T and its identifiability using increasingly truncated durations of brain data. The value of V_T was stably identified after ~60 min of scanning and had good identifiability (*i.e.*, low percentage values) after ~70 min (Fig. 4).

Although the identifiability of V_T was good after 150 min of scanning (SE ~5% or less), we observed a high intersubject variability of V_T among the initial eight subjects (~61%). In contrast, the intersubject variability of brain uptake$_{40–80}$ was much lower (17%). V_T is calculated from both brain and plasma data. Although high intersubject variability of V_T might reflect actual variations in CB_1 receptor density in this population, we wondered if it was caused by noise in the measurements of either brain radioactivity or the concentration of [^{11}C]MePPEP in plasma. To assess the relative contributions of noise in brain and plasma data, we performed a retest study and assumed that the concentration of CB_1 receptors in brain and the clearance of radioligand from plasma were unchanged in each subject within a single day. Furthermore, although V_T appeared to be stably determined after ~60 min, we increased the imaging time of both the test and retest scans to 210 min to see if values of V_T both remained stable during this extra 60 min of imaging and reduced its variability.

The high intersubject variability of V_T might have also been caused by variations in plasma free fraction of [^{11}C]MePPEP. However, the intersubject variability of V_T / f_P was virtually identical to that of V_T in all eight brain regions of the 12 subjects in whom f_P was measured, using 150 min of image data. Thus, correction of V_T for individual values of plasma protein binding neither increased nor decreased intersubject variability.

Retest variability using 210 min of scan data

Similar to the results using 150 min of scan data, those from 210 min showed higher intersubject variability of V_T (~39%) than of brain uptake$_{40–80}$ (~15%). In a similar manner, the retest variability (*i.e.*, within subject) of V_T (~15%) was nearly twice that of brain uptake$_{40–80}$ (~8%; Table 3). However, the retest variability of the plasma measurements was extraordinarily high. The exposure to the brain is the area under the curve (AUC) of [^{11}C]MePPEP in arterial plasma extrapolated to infinity. The retest variability of plasma AUC was ~58%, and the ICC was −0.02. Since V_T equals the ratio of brain AUC to plasma AUC, we suspect that the primary cause of the high intersubject variability of V_T was uncertainty or noise in the measurement of plasma AUC. Furthermore, the terminal clearance of [^{11}C]MePPEP was very slow (half-life of 3700 min (see above)), several times the physical half-life of ^{11}C itself (20.4 min).

Similar to the data from 150 min of scanning, we increasingly truncated the data from 210 min to determine minimal scan duration to obtain stable values of V_T. We again found that V_T was relatively stable after ~60 min and had good identifiability after ~80 min (Fig. 4). We compared the V_T, retest variability, intersubject variability, and ICC acquired after 210 min to that of the data truncated to 150 min within the same subjects and found that they were essentially identical (change ≤3%).

Can brain uptake substitute for distribution volume?

Brain uptake not corrected for plasma measurements has been used with another radioligand to measure CB_1 receptor availability in human brain (Burns et al., 2007; Van Laere et al., 2008). Furthermore, we found that the intersubject variability and retest variability of brain uptake was much better than that of V_T. To evaluate whether brain uptake is an accurate measurement of receptor density, we simulated increased and decreased receptor densities by corresponding changes in k_3. We used the average input function and rate constants for prefrontal cortex from the 17 subjects scanned for 150 min. Brain uptake was calculated for three time intervals: 40–80, 0–210, and 150–180 min.

Brain uptake for all three time intervals followed the pattern of increasing or decreasing receptor density but underestimated the change (Fig. 5). For example, a 50% increase in receptor density yielded only 13–30% increase of brain uptake during these three time intervals, while V_T increased by 45%. In addition, a 50% decrease in receptor density yielded a 25–44% decrease of brain uptake during these three time intervals, while V_T decreased by 45%.

In turn, we wanted to know the impact that good precision and poor accuracy has on using brain uptake to measure changes in CB_1 receptor density, so we calculated the expected number of subjects needed to detect these simulated outcome measurements. Estimation of sample sizes for a two-tailed independent samples *t*-test was made assuming $\alpha = 0.05$ (probability of type I error) and $\beta = 0.20$ (probability of type II error, *i.e.*, power of 80%). Intersubject variability from our measurements from 17 subjects was used to estimate the pooled standard deviation of outcome (V_T and brain uptake), and results from

Table 3
Retest variability of brain uptake and distribution volume in 8 subjects scanned for 210 min.

Region	Brain uptake$_{40–80}$[a]				Distribution volume			
	Conc. (SUV)	Intersubject variability	Retest variability	ICC	V_T (mL·cm^{-3}) SE	Intersubject variability	Retest variability	ICC
Prefrontal cortex	2.94	17%	8%	0.78	17.8 ± 6.4 2%	36%	15%	0.91
Occipital cortex	2.95	16%	8%	0.75	12.3 ± 4.2 2%	34%	12%	0.93
Hippocampus	2.21	13%	7%	0.73	18.5 ± 9.4 5%	51%	21%	0.81
Putamen	3.60	17%	8%	0.75	22.4 ± 7.8 3%	35%	17%	0.87
Thalamus	2.46	15%	8%	0.75	9.6 ± 3.3 3%	34%	11%	0.94
Cerebellum	2.47	18%	8%	0.79	11.7 ± 3.4 3%	29%	16%	0.82
Pons	1.98	19%	8%	0.85	5.9 ± 1.3 6%	22%	13%	0.82
White matter	1.13	13%	8%	0.71	8.7 ± 7.0 –	80%	108%	0.15

Brain uptake and V_T reflect only the baseline scan from 8 healthy subjects (mean ± SD).
The identifiability of V_T is inversely related to the standard error (SE). For each brain region, the SE is expressed as percent and is listed below the variable itself.
Intersubject variability is the SD divided by the mean, and is expressed as percent.
Retest variability is the absolute value of the difference between test and retest, divided by their mean, and is expressed as percent.
[a] Brain uptake is the average radioactivity from 40 to 80 min after injection.

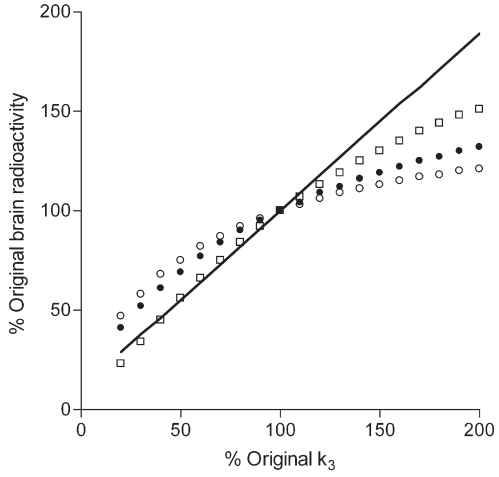

Fig. 5. Simulated changes in brain uptake with variations of receptor density. The average individual kinetic parameters from the prefrontal cortex were used to simulate expected changes in brain uptake from 40 to 80 (○), 0 to 210 (●), and 150 to 180 (□) min. Changes in receptor density were simulated by varying the value of k_3 from its mean value (set at 100% on the *x*-axis). As expected, the value of V_T (shown by a line which has a *y*-intercept equal to K_1 / k_2) is directly proportional to changes in k_3.

our simulations of varying receptor density determined the measured difference to be detected. We found that 25 subjects would be needed when measuring brain uptake$_{40–80}$ *vs.* 26 subjects when measuring V_T if a 50% increase of receptor density is expected. However, 8 subjects would be needed when measuring brain uptake$_{40–80}$ *vs.* 26 subjects when measuring V_T if a 50% decrease of receptor density is expected.

Discussion

The purpose of this study was to evaluate the ability of [^{11}C]MePPEP to quantify CB_1 receptors in human brain in regard to several characteristics, including minimal time necessary to scan subjects, retest variability, and intersubject variability. [^{11}C]MePPEP readily entered human brain with high uptake (>3.0 SUV) and had a distribution consistent with that of CB_1 receptors (Glass et al., 1997). The values of distribution volume had good identifiability (SE<10%) and were relatively stable after about 60 min of imaging. We found that scanning up to 210 min provided quantifiable data but did not significantly improve the identifiability or retest variability of distribution volume measured using the initial 150 min of data. We compared brain uptake and the more complicated but theoretically more accurate distribution volume, which corrects for exposure of the parent radioligand to brain. The retest variability of brain uptake$_{40–80}$ (~8%) was better than that of distribution volume (~15%), which might be expected since V_T includes multiple variables and calculations. Surprisingly, the intersubject variability of V_T (~52% COV) was more than three times that of brain uptake$_{40–80}$ (~16% COV). With the current data, we cannot determine whether brain uptake or distribution volume is the more accurate measure of CB_1 receptor density, since we do not know the actual intersubject variability of CB_1 receptors in this group of subjects. Nevertheless, we suspect that noise in measurement of the input function of distribution volume decreased our precision in measuring V_T.

Advantages and limitations of [^{11}C]MePPEP

[^{11}C]MePPEP had such high uptake and retention in brain that it could be meaningfully measured for 210 min, which is greater than ten times the radioactive half-life of ^{11}C. Distribution volume was well identified (SE ~5%), showed good time stability after ~60 min, and had good reliability on test–retest study (ICC ~0.90). In addition, the short half-life of the ^{11}C label allowed us to perform two scans in a subject per day.

Our assessment also uncovered several limitations of [^{11}C]MePPEP. The washout of radioactivity from brain was slow and difficult to quantify. Although distribution volume is typically defined using rate constants, it may be more easily conceptualized as the ratio of two areas under the curve (AUC) extrapolated to infinite time. Distribution volume equals AUC in brain divided by AUC of parent radioligand in plasma. The slow washout from brain decreased the precision to extrapolate AUC in brain to infinite time. Even after 210 min we had observed only about one third of the total AUC of brain. The slow washout was caused by the high affinity of the radioligand ($K_D = 0.14 \pm 0.03$ nM in human cerebellum, unpublished data) and by the high density of CB_1 receptors in brain. In fact, we estimate that the density of CB_1 receptors, if evenly distributed in the entire brain, would be more than six times that of dopamine D_2 receptors in striatum. The high density of CB_1 receptors allowed rapid rebinding of the radioligand, creating a "synaptic barrier" that impedes exit of the radioligand from brain to plasma (Frost and Wagner, 1984).

While high concentrations of radioactivity in brain allowed us to image for 210 min, low concentrations in plasma restricted our measuring the input function to only the initial 120 min. The low concentration of the radioligand was due to distribution and clearance as well as physical decay of ^{11}C. Measurements of such low concentrations introduced noise in the input function, which then decreased the precision of V_T. A fluorine-18 labeled version of [^{11}C]MePPEP may permit a longer acquisition time from both brain and plasma, and the resulting V_T might be more precise.

[^{11}C]MePPEP is also flawed by having very low free fraction in plasma (f_P). Since only free radioligand in plasma can cross the blood–brain barrier, distribution volume should be corrected for (*i.e.,* divided by) f_P to more accurately measure CB_1 receptor density. We wondered whether correcting for f_P would decrease retest and intersubject variability of distribution volume. Correcting both brain uptake and V_T for f_P neither increased nor decreased retest or intersubject variability. The mean value of f_P for [^{11}C]MePPEP was 0.05%, which corresponds to a bound fraction of 99.95%. The impact would seem insignificant if the bound fraction increased from 99.95% to 99.97%. However, such a change would nearly halve the value of f_P to 0.03%, and would then nearly double the corrected value of V_T. We suspect that the low values of f_P will be problematic in clinical studies, because apparently minute differences may exist between groups. Additionally, if [^{11}C]MePPEP is used to measure receptor occupancy by medications, investigators should confirm that the medications do not change the plasma protein binding of the radioligand.

Precision and accuracy affect sample sizes for clinical studies

Our current results demonstrate that brain uptake has greater precision than V_T, but brain uptake is theoretically less accurate. We use "precision" most narrowly in reference to retest reproducibility, with the assumption that the density and affinity of receptors do not change between scans. In this study, we also indirectly gauge precision by intersubject variability, since a less precise measurement will have greater standard deviation in the population. In comparison to distribution volume, we found brain uptake had greater precision because it had better retest reproducibility and as suggested by its lower intersubject variability. However, high intersubject variability merely suggests poor precision, since it inseparably incorporates both precision and accuracy.

We use "accuracy" to refer to the theoretically correct measurement. For example, distribution volume provides a more accurate measure of receptor density than brain uptake, because distribution volume corrects for exposure of the brain to the concentration of radioligand in plasma. The concentration in plasma differs between

subjects based on variations in distribution, metabolism, and excretion of the radioligand. Accuracy is more difficult to measure than precision, since we do not know the actual density of CB_1 receptors in these subjects. In this study, we indirectly assessed accuracy in two ways. First, for the retest study, an ICC value of 1 is associated with greatest accuracy. Second, for measurement of minimal time to calculate distribution volume, a time-stable value is consistent with an accurate measurement that is not contaminated by radiometabolites. Nevertheless, both ICC and time stability are merely consistent, with but do not prove, accuracy. For example, our prior *ex vivo* study of [^{11}C]MePPEP in rat brain showed that distribution volume can also be stable over time even in the presence of a radiometabolite, if its percentage of total radioactivity in brain is constant (Terry et al., 2008).

What is the relative sensitivity of brain uptake and distribution volume to discern changes in CB_1 receptor density between groups, and what sample sizes would be required? To estimate sample sizes, we assumed that distribution volume (V_T) provides the accurate measure of receptor density, though we found it to be less precisely measured than brain uptake$_{40–80}$, and then simulated the effect of changing receptor density on brain uptake. We found that brain uptake underestimated both increases and decreases in receptor density, and that this underestimation was more severe for increased than decreased receptor density (Fig 5).

For example, a 50% decrease in receptor density would be erroneously measured as only 25% decrease of brain uptake$_{40–80}$. However, because of its greater precision, brain uptake$_{40–80}$ would require only 8 subjects per group, while V_T would require 26 per group to achieve the same statistical endpoint (significance level = 0.05 and power = 80%). In contrast, a 50% increase of receptor density would be erroneously measured as only 13% increase of brain uptake$_{40–80}$. Despite its greater precision, brain uptake$_{40–80}$ would require 25 subjects per group, while V_T would require 26 per group to achieve the same statistical endpoint. In summary, the effects of precision and accuracy have differential effects on the relative sample sizes required for brain uptake and distribution volume.

Brain uptake$_{0–210}$ was more sensitive than brain uptake$_{40–80}$ in these simulations, however brain uptake$_{150–180}$ had superior sensitivity to either time period, reflecting that radioactivity in brain is more dependent on k_3 at later times during the scan. While brain uptake$_{150–180}$, or perhaps even later time frames, may be more sensitive than brain uptake$_{40–80}$ in measuring changes in k_3, the added noise at those later time frames may cause their measurements to be less precise.

Based on these results, we recommend using brain uptake$_{40–80}$ as an outcome measure only for within subject studies (*e.g.,* receptor occupancy), since brain uptake is more reproducible than V_T. However, we recommend that V_T be used for between subject studies (patients *vs.* healthy subjects), because it is more accurate than brain uptake. Furthermore, our simulations on the effects of accuracy and precision are merely predictions, which need validation from larger sample sizes of both patients and healthy subjects.

Comparison with two other CB_1 radioligands

The first two successful radioligands to image CB_1 receptors in human brain were [^{18}F]MK-9470 (Burns et al., 2007) and [^{11}C]JHU75528 (Horti et al., 2006). Assessed by peak brain uptake, [^{18}F]MK-9470 has been used to measure receptor occupancy by a nonradioactive inverse agonist (taranabant, Burns et al., 2007), to show an age-related increase of CB_1 receptors in women but not in men (Van Laere et al., 2008), and to find an association of CB_1 receptor density with novelty seeking personality (Van Laere et al., 2009). Compared to [^{18}F]MK-9470, [^{11}C]MePPEP has about 2.5 times greater uptake in human brain (~1.4 *vs.* 3.6 SUV) but comparable retest variability and intersubject variability when brain uptake is used as the outcome measure. However, the washout of radioactivity from brain for [^{18}F]MK-9470 appears to be even slower than that for [^{11}C]MePPEP. If so, measurement of distribution volume for [^{18}F]MK-9470 may be quite problematic and have low identifiability and poor time stability.

Results using [^{11}C]JHU75528 (also called [^{11}C]OMAR) have been published from baboons as a paper (Horti et al., 2006) and from humans as an abstract (Wong et al., 2008). [^{11}C]JHU75528 has low to moderate uptake in baboon brain (peak uptake of ~1.0 SUV) and can be displaced by nonradioactive ligands. The peak uptake in brain of [^{11}C]MePPEP is higher than that of [^{11}C]JHU75528: ~4–6 times higher in monkey and ~2 times higher in human. Quantification of [^{11}C]JHU75528 using arterial input function has not been fully described.

In summary, although the brain uptake of [^{11}C]MePPEP is greater than that of [^{18}F]MK-9470 and [^{11}C]JHU75528, the more important comparisons may well be resolved only after detailed kinetic analysis are reported for all three radioligands.

Conclusion

[^{11}C]MePPEP has high brain uptake and regional distribution in human brain consistent with that of CB_1 receptors. In addition, by standard measures, [^{11}C]MePPEP provides good quantitation of receptor density using both brain and plasma data — *i.e.*, distribution volume is well identified and has relatively stable values after ~60 min of imaging. Nevertheless, the high variability of distribution volume among subjects suggests that it is not as precisely measured as suggested by identifiability. For within subject studies (*e.g.*, receptor occupancy by medications), peak uptake of [^{11}C]MePPEP will be useful, since this outcome measure showed good retest variability. For between subject studies (*e.g.*, patients *vs.* healthy subjects), distribution volume is theoretically superior to peak uptake. However, the plasma measurements required to calculate distribution volume add moderate noise to this outcome measure. Thus, between subject studies must have adequate sample sizes to detect differences because of the moderately high retest and intersubject variability of distribution volume measured with [^{11}C]MePPEP.

Acknowledgments

We thank Ed Tuan, Pavitra Kannan, Kimberly Jenko, and Kacey Anderson for measurements of radioligand in plasma; Yi Zhang for preparation of [^{11}C]MePPEP; Desiree Araneta, William C. Kreisl, Barbara Prewitt, and the NIH PET Department for imaging; and PMOD Technologies for providing its image analysis and modeling software. This research was supported by a Cooperative Research and Development Agreement with Eli Lilly and by the Intramural Program of NIMH (projects # Z01-MH-002852-04 and #Z01-MH-002793-04). Jussi Hirvonen was supported by personal grants from The Academy of Finland, The Finnish Cultural Foundation, The Finnish Foundation for Alcohol Studies, The Finnish Medical Foundation, The Instrumentarium Foundation, The Jalmari and Rauha Ahokas Foundation, The Paulo Foundation, The Research Foundation of Orion Corporation, and The Yrjö Jahnsson Foundation.

References

Abood, M.E., Ditto, K.E., Noel, M.A., Showalter, V.M., Tao, Q., 1997. Isolation and expression of a mouse CB_1 cannabinoid receptor gene. Comparison of binding properties with those of native CB_1 receptors in mouse brain and N18TG2 neuroblastoma cells. Biochem. Pharmacol. 53, 207–214.

Akaike, H., 1974. A new look at the statistical model identification. IEEE Trans. Automat. Contr. AC19 716–723.

Bevington, P.R., Robinson, D.K., 2003. Data Reduction and Error Analysis for the Physical Sciences, 3rd ed. McGraw-Hill, New York.

Burger, C., Mikolajczyk, K., Grodzki, M., Rudnicki, P., Szabatin, M., Buck, A., 1998. JAVA tools quantitative post-processing of brain PET data. J. Nucl. Med. 39(Suppl.), 277P.

Burns, H.D., Van Laere, K., Sanabria-Bohorquez, S., Hamill, T.G., Bormans, G., Eng, W.S., Gibson, R., Ryan, C., Connolly, B., Patel, S., Krause, S., Vanko, A., Van Hecken, A., Dupont, P., De Lepeleire, I., Rothenberg, P., Stoch, S.A., Cote, J., Hagmann, W.K., Jewell, J.P., Lin, L.S., Liu, P., Goulet, M.T., Gottesdiener, K., Wagner, J.A., de Hoon, J., Mortelmans, L., Fong, T.M., Hargreaves, R.J., 2007. [^{18}F]MK-9470, a positron emission tomography (PET) tracer for *in vivo* human PET brain imaging of the cannabinoid-1 receptor. Proc. Natl. Acad. Sci. U. S. A. 104 (23), 9800–9805.

Carson, R.E., 1986. Parameter estimation in positron emission tomography. In: Phelps, M.E., Mazziotta, J.C., Schelbert, H.R. (Eds.), Positron Emission Tomography and Autoradiography: Principles and Applications for the Brain and Heart. Raven Press, New York, pp. 347–390.

Donohue, S.R., Krushinski, J.H., Pike, V.W., Chernet, E., Phebus, L., Chesterfield, A.K., Felder, C.C., Halldin, C., Schaus, J.M., 2008. Synthesis, ex vivo evaluation, and radiolabeling of potent 1,5-diphenylpyrrolidin-2-one cannabinoid subtype-1 receptor ligands as candidates for in vivo imaging. J. Med. Chem. 51 (18), 5833–5842.

Eggan, S.M., Hashimoto, T., Lewis, D.A., 2008. Reduced cortical cannabinoid 1 receptor messenger RNA and protein expression in schizophrenia. Arch. Gen. Psychiatry 65 (7), 772–784.

Frost, J.J., Wagner, H.N., 1984. Kinetics of binding to opiate receptors in vivo predicted from in vitro parameters. Brain Res. 305 (1), 1–11.

Gandelman, M.S., Baldwin, R.M., Zoghbi, S.S., Zea-Ponce, Y., Innis, R.B., 1994. Evaluation of ultrafiltration for the free-fraction determination of single photon emission computed tomography (SPECT) radiotracers: beta-CIT, IBF, and iomazenil. J. Pharm. Sci. 83 (7), 1014–1019.

Gatley, S.J., Gifford, A.N., Volkow, N.D., Lan, R., Makriyannis, A., 1996. ^{123}I-labeled AM251: a radioiodinated ligand which binds in vivo to mouse brain cannabinoid CB1 receptors. Eur. J. Pharmacol. 307 (3), 331–338.

Gatley, S.J., Lan, R., Volkow, N.D., Pappas, N., King, P., Wong, C.T., Gifford, A.N., Pyatt, B., Dewey, S.L., Makriyannis, A., 1998. Imaging the brain marijuana receptor: development of a radioligand that binds to cannabinoid CB1 receptors in vivo. J. Neurochem. 70 (1), 417–423.

Gazzerro, P., Caruso, M.G., Notarnicola, M., Misciagna, G., Guerra, V., Laezza, C., Bifulco, M., 2007. Association between cannabinoid type-1 receptor polymorphism and body mass index in a southern Italian population. Int. J. Obes. (Lond.) 31 (6), 908–912.

Glass, M., Dragunow, M., Faull, R.L., 1997. Cannabinoid receptors in the human brain: a detailed anatomical and quantitative autoradiographic study in the fetal, neonatal and adult human brain. Neuroscience 77 (2), 299–318.

Hawkins, R.A., Phelps, M.E., Huang, S-C., 1986. Effects of temporal sampling, glucose metabolic rates, and disruptions of the blood–brain barrier on the FDG model with and without a vascular compartment: studies in human brain tumors with PET. J. Cereb. Blood Flow Metab. 6, 170–183.

Horti, A.G., Fan, H., Kuwabara, H., Hilton, J., Ravert, H.T., Holt, D.P., Alexander, M., Kumar, A., Rahmim, A., Scheffel, U., Wong, D.F., Dannals, R.F., 2006. ^{11}C-JHU75528: a radiotracer for PET imaging of CB_1 cannabinoid receptors. J. Nucl. Med. 47 (10), 1689–1696.

Howlett, A.C., Barth, F., Bonner, T.I., Cabral, G., Casellas, P., Devane, W.A., Felder, C.C., Herkenham, M., Mackie, K., Martin, B.R., Mechoulam, R., Pertwee, R.G., 2002. International Union of Pharmacology. XXVII. Classification of cannabinoid receptors. Pharmacol. Rev. 54 (2), 161–202.

Imaizumi, M., Kim, H.J., Zoghbi, S.S., Briard, E., Hong, J., Musachio, J.L., Ruetzler, C., Chuang, D.M., Pike, V.W., Innis, R.B., Fujita, M., 2007. PET imaging with [^{11}C]PBR28 can localize and quantify upregulated peripheral benzodiazepine receptors associated with cerebral ischemia in rat. Neurosci. Lett. 411 (3), 200–205.

Innis, R.B., Cunningham, V.J., Delforge, J., Fujita, M., Gjedde, A., Gunn, R.N., Holden, J., Houle, S., Huang, S-C., Ichise, M., Iida, H., Ito, H., Kimura, Y., Koeppe, R.A., Knudsen, G.M., Knuuti, J., Lammertsma, A.A., Laruelle, M., Logan, J., Maguire, R.P., Mintun, M.A., Morris, E.D., Parsey, R., Price, J.C., Slifstein, M., Sossi, V., Suhara, T., Votaw, J.R., Wong, D.F., Carson, R.E., 2007. Consensus nomenclature for *in vivo* imaging of reversibly binding radioligands. J. Cereb. Blood Flow Metab. 27, 1533–1539.

Jones, D., 2008. End of the line for cannabinoid receptor 1 as an anti-obesity target? Nat. Rev. Drug Discov. 7 (12), 961–962.

Terry, G., Liow, J-S., Chernet, E., Zoghbi, S.S., Phebus, L., Felder, C.C., Tauscher, J., Schaus, J.M., Pike, V.W., Halldin, C., Innis, R.B., 2008. Positron emission tomography imaging using an inverse agonist radioligand to assess cannabinoid CB_1 receptors in rodents. Neuroimage 41 (3), 690–698.

Tzourio-Mazoyer, N., Landeau, B., Papathanassiou, D., Crivello, F., Etard, O., Delcroix, N., Mazoyer, B., Joliot, M., 2002. Automated anatomical labeling of activations in SPM using a macroscopic anatomical parcellation of the MNI MRI single-subject brain. Neuroimage 15 (1), 273–289.

Van Laere, K., Goffin, K., Casteels, C., Dupont, P., Mortelmans, L., de Hoon, J., Bormans, G., 2008. Gender-dependent increases with healthy aging of the human cerebral cannabinoid-type 1 receptor binding using [^{18}F]MK-9470 PET. Neuroimage 39 (4), 1533–1541.

Van Laere, K., Goffin, K., Bormans, G., Casteels, C., Mortelmans, L., de Hoon, J., Grachev, I., Vandenbulcke, M., Pieters, G., 2009. Relationship of type 1 cannabinoid receptor availability in the human brain to novelty-seeking temperament. Arch. Gen. Psychiatry 66 (2), 196–204.

Wong, D.F., Kuwabara, H., Horti, A.G., Kumar, A., Brasic, W.Y., Alexander, M., Raymont, V., Galecki, J., Charlotte, M., Cascella, N., 2008. PET imaging of cannabinoid CB_1 type receptors in healthy humans and patients with schizophrenia using [^{11}C]OMAR. NeuroImage Neuroreceptor Mapping 2008, T51.

Yasuno, F., Brown, A.K., Zoghbi, S.S., Krushinski, J.H., Chernet, E., Tauscher, J., Schaus, J.M., Phebus, L.A., Chesterfield, A.K., Felder, C.C., Gladding, R.L., Hong, J., Halldin, C., Pike, V.W., Innis, R.B., 2008. The PET radioligand [^{11}C]MePPEP binds reversibly and with high specific signal to cannabinoid CB_1 receptors in nonhuman primate brain. Neuropsychopharmacology 33 (2), 259–269.